

Christopher Holsonback, Tyler Webb, Dr. Thomas Kiehne, P.E., Dr. Carolyn Conner
Seepersad

System-Level Modeling and Optimal Design of an All-Electric Ship Energy Storage Module

INTRODUCTION

Conventional naval surface ships rely on large mechanical drive systems for propulsion. These systems typically include gas turbines as the prime movers, large reduction gearboxes, and long shafts to connect the gearboxes and propellers. For example, each of the *Arleigh Burke* class (DDG 51) ships is equipped with seven gas turbines: four GE LM2500's strictly dedicated to propulsion and three Allison 501-K34's for ship service power (Ewing et al. 1995). Of the total installed power, over 90% is reserved for propulsion. Since recent studies have shown that these ships spend very little time at full speed, this inflexibility of power distribution results in a significant reduction in system efficiency (Surko and Osbourne 2005). Further, the mechanical drive system requires elaborate gearing or variable-pitch propellers to reverse the ship, both of which increase cost and complexity and negatively affect fuel efficiency (Doerry and Davis 1994). Finally, the mechanical connection between propeller and turbine can impose undesirable transients on the prime movers, which may increase fuel and maintenance costs during the life of the ship.

Future naval warships will be powered through a combined propulsion and electrical power distribution system, currently conceptualized as the integrated fight-through power (IFTP) system. In this revolutionary architecture, the vast majority of ship systems will be powered electrically. All of the prime movers onboard the ship will be coupled to generators and their singular purpose will be to create electrical power. In general fewer prime movers will be needed, reducing acquisition costs. Electromagnetic motors will propel the ship, possibly outside of the ship hull in azimuthing podded propulsors (Young, Newell, and Little 2001). Releasing the prime movers from ship

propulsion will allow for the removal of the traditional mechanical drive system, freeing valuable internal volume and dramatically increasing the electrical power available for other systems such as future electric weapons and advanced sensors (McCoy 2002). Further, maintaining the prime movers at their most efficient loading and isolating them from propulsion dynamics will generate fuel and maintenance cost savings over the life of the ship. These characteristics and capabilities broadly define the future all-electric ship (AES) (Doerry et al. 1996).

NEED FOR ENERGY STORAGE ON THE AES

An enabling capability of the AES will be the ability to survive situations where power distribution and/or power production is lost. The former is the goal of dynamic reconfiguration; the latter is the goal of energy storage. Because of the decoupling of the prime movers from the propulsion system, more electrical energy can be created than is consumed by the ship systems during the vast majority of ship missions. This excess energy can be stored in some type of energy storage module (ESM) and returned to the system when needed. This ability may help the AES avoid a devastating shipwide or zonal electrical failure.

Current surface ships utilize energy storage in the form of uninterruptible power supplies (UPS) for critical equipment such as navigational radar, weapons and sensors, emergency lights, and internal communications (Little, Young, and Newell 2001; Newell and Young 2001). In general, UPS have relatively low capacity and are located near or within the load they are supporting. Extending the idea of UPS, one could envision an AES where each electrical load had its own dedicated UPS.

However, this solution represents an undue amount of redundancy and implies that all loads are equally critical, which is untrue (Amy 2002). A more elegant solution involves fully integrating the ESM into the zonal IFTP system. With zonal energy storage (ZES), each zone will contain an ESM that is customized to the needs of the zone in terms of voltage, peak power, capacity, signal quality, etc. (Little, Young, and Newell 2001; Newell and Young 2001). Because of its distributed nature, ZES requires that the technology chosen to power the ESM be relatively insensitive to undisciplined charging and discharging, have a simple and reliable method for determining the amount of energy stored, and have limited maintenance requirements (Donaldson 2002). This is a significant deviation from the characteristics of conventional bulk energy storage, as seen in modern submarines, aircraft carriers, and underwater autonomous vehicles (Donaldson and Williamson 2005; Sette and Spina 2002; Szyborski 2002).

Beyond survivability, incorporating energy storage into the AES will increase overall system efficiency, much like it does in utility power plants. Traditional utility plants must balance generation against demand and losses at each instant in time (Price 1999). This frequently results in low utilization and idling of equipment to hedge against abrupt increases in demand. More advanced utilities, especially those that depend upon unpredictable renewable energy sources, utilize energy storage in both high-power and high-energy forms. High-power devices such as capacitors, flywheels, and superconducting magnetic energy storage (SMES) are used to improve system reliability. High-energy devices such as pumped hydro and compressed air energy storage (CAES) are generally used for load leveling and arbitrage (Nourai 2002). In a similar way, energy storage on the AES would serve to increase the overall efficiency of the system, provide redundancy and emergency power, and may allow for the reduction in the number of prime movers (Donaldson 2002).

Another unique capability of the AES is that of single-generator operation (SGO). During

periods of low, relatively stable electrical demand, a single gas turbine generator set (GTGS) may be used to power the entire ship. In case a single GTGS cannot provide the power demanded by the system, SGO implies the minimum number of GTGSs will be used. It has been argued that SGO is only reasonable during benign, open-water patrolling conditions, due to multiple generators being needed in most other situations (Newell and Young 2001). The goal of SGO is to run the prime mover near full load, where it is most efficient. Shutting down unneeded GTGS saves maintenance and fuel expense, reducing life-cycle costs.

The risk inherent to SGO is that of a dark-start emergency, whereby the ship loses all power production capability due to an emergency such as a ground fault that isolates the GTGS from the ship electrical system. During a dark-start, another prime mover must be started and begin power production as soon as the ground fault is cleared. In the mean time, power must be maintained to critical loads such as navigation, sensors, emergency lighting, steering, backup GTGS startup, and potentially some propulsion (Hudson and Ross 1998). This represents a clear opportunity for energy storage and in fact it has been argued that without energy storage, SGO is infeasible (Doerry et al. 1996).

In summary, incorporating energy storage into the AES will serve to increase system redundancy, survivability, availability, and efficiency. Although the quantity and duration of stored energy is still subject to debate, the technologies capable of meeting the stringent demands of naval systems are relatively few. The remainder of this paper includes an assessment of commercially available energy storage technologies, the selection of those technologies that are most likely to be included on a future AES, the system-level sizing of an ESM composed of each technology depending on specified energy and peak-power demands, and a discussion of the results of the analysis.

The overarching goal of this assessment is to determine which energy storage technologies will require the smallest volume and weight, while meeting the energy and power demands of

the AES. Due to the system-level nature of this analysis, the results will not address the issue of zonal versus bulk energy storage due to a lack of the requisite zonal load data. Further, only general-use energy storage will be examined. Dedicated energy storage systems, such as for pulsed weapons or sensors, may have very specific design metrics that are not descriptive of the energy or peak-power needs of the AES as a whole, and therefore will not be considered. Finally, the field of energy storage technologies will be limited to those that are mature-enough to be included on an AES within approximately five years.

ASSESSMENT & MODELING OF ENERGY STORAGE TECHNOLOGIES

Energy Storage Technology Assessment

Recognizing previous assessments of the energy storage options for a future AES, the following technologies were deemed sufficiently mature, robust, and energy and power dense to be included in the preliminary assessment (Lipscombe, Davies, and Bolton 1998; Hudson and Ross 1998; Baker and Benstead 2005):

- Batteries—lead-acid, valve-regulated lead-acid (VRLA), Zebra, and lithium-ion (Li-ion) chemistries
- Flywheels
- Superconducting Magnetic Energy Storage (SMES)
- Supercapacitors
- Compressed Air Energy Storage (CAES)

A Pugh chart was created to help quantify the relative advantages and disadvantages of the competing energy storage technologies, and is presented in Figure 1. Several general comparisons of energy storage technologies from the literature provided data for the Pugh chart but are not referenced in the figure (Schainker 2004; Lipscombe, Davies, and Bolton 1998).

The results consist of a comparison of the available technologies relative to a datum, lead-acid batteries. The relative comparison is influenced by factors such as the importance placed on each metric and the availability of

useful, validated data for a particular technology. However, a brief explanation of the scores may help support the authors' conclusions. Lead-acid batteries were chosen as the datum due to the U.S. Navy having significant experience with this medium (Donaldson and Williamson 2005). In fact, conventional lead-acid batteries have been relied upon for primary power on submarines while submerged for over a century (Donaldson 2002). Li-ion technology shows several clear advantages over lead-acid, especially in power and energy density, lifetime, and round-trip efficiency. Due to their somewhat lower specific power and energy, ZEBRA batteries have until recently been used primarily in stationary applications. The advantages of the ZEBRA cells occur mostly in lower-weighted metrics, and subsequently they fail to demonstrate a clear advantage over the datum. VRLA batteries have significantly improved safety, durability, and maintenance requirements, but otherwise exhibit the characteristics of flooded cells.

Supercapacitors have extremely high power capability and much longer lifetimes, but at the cost of low energy density, high self discharge, and insufficient discharge times. Flywheels show significant advantages in the areas of power capability, lifetime, cyclical efficiency, and ease of monitoring, with primary shortcomings in ability to store energy, cost, and need for auxiliary equipment. However, as the technology matures it is expected that the energy storage characteristics will improve in an evolutionary way. SMES exhibits many of the same advantages as supercapacitors with the additional disadvantages of high cost and significant auxiliary equipment. In addition, its lack of robustness to a hostile or unpredictable environment effectively relegates SMES to stationary applications. Finally, like lead-acid technology, the Navy also has considerable experience with compressed air systems. In fact, they are currently used to start gas turbines on naval ships. However, because of the significant auxiliary systems and volume needed for significant energy storage, CAES does not fit in the framework of ZES and is much more suited to land-based applications. Further, the

Energy Storage Options	Metrics														Scoring			References
	Energy Density [kWh/m ³]	Specific Energy [kJ/kg]	Specific Power [W/kg]	Power Range [MW]	Discharge Time @ Rated Power	Initial Cost [\$]	Through-Life Cost [\$]	Cycles per Life [#]	State of Charge Monitoring	Efficiency [%]	Aux Systems	Safety Issues	Robustness/Durability	Maturity	M ⁺	M ⁻	Total M	
Importance	5	5	5	4	5	4	3	4	4	3	3	3	3	4				
Lead-Acid Batteries	40-100	108-180	200-400	10	hours	Low	High	1000	Hard	70%	Low	High	Med	High	Datum			
Li-Ion Batteries	+	+	+	0	0	-	+	+	+	++	0	0	0	-	32	-8	24	Saft et al 1999
Zebra batteries	+	-	-	0	0	-	+	+	0	+	0	+	0	-	18	-18	0	Dustmann 2004
VRLA Batteries	0	+	0	0	0	-	+	0	0	0	0	+	+	0	14	-4	10	
Super Capacitors	--	--	++	+	--	0	+	++	+	++	0	+	+	0	41	-30	11	Barker 2002
Flywheels	-	-	++	+	-	-	+	++	++	+	-	+	0	-	39	-25	14	
SMES	--	--	++	+	--	--	-	+	+	++	--	+	-	--	31	-58	-27	
CAES	-	-	+	-	-	0	0	+	+	+	--	0	0	0	20	-25	-5	Nourai 2002

FIGURE 1. Pugh Chart of Energy Storage Technologies

inclusion of CAES would run counter to the goal of reducing the number of hydraulic and pneumatic systems onboard the AES by the electrification of auxiliaries (Newell, Mattick, and Hodge 1999).

The Pugh chart and foregoing discussion make a cogent argument that Li-ion batteries and flywheels are the most promising technologies for an AES ESM. As discussed previously, ZES requires technologies that are insensitive to undisciplined charging and discharging, have a simple and reliable method for determining the amount of energy stored, and have limited maintenance requirements (Donaldson 2002). Flywheels and Li-ion batteries can fit within this framework if fitted with the proper control and monitoring equipment. The following section discusses flywheels and Li-ion batteries in more depth.

Li-Ion Batteries

Li-ion battery technology has made significant advancements over the past decade, and revolutionary improvements appear on the horizon through nanotechnology (Amatucci and Badway 2002). Li-ion batteries exhibit a higher terminal voltage, better cyclical efficiency, higher continuous and pulsed current limits, higher energy and power densities, and better lifetime characteristics than most other

secondary battery chemistries. One of Li-ion's main advantages is that, unlike other rechargeable cells, they do not readily develop a "memory," whereby, as a result of shallow charge and discharge cycles, a fully charged cell responds to loading as though it has very little capacity. In fact, Li-ion cells exhibit the best characteristics when frequently recharged. Subsequently, the terminal voltage of a Li-ion battery is generally a good indication of the remaining capacity, which simplifies state-of-charge monitoring (Pelletier and Pommereau 2005). Finally, Li-ion cells do not generate combustible or flammable gasses during normal cycling as conventional lead-acid cells do.

Regardless, Li-ion batteries have their share of drawbacks. The most prominent issue with Li-ion cells is that they can vent liquid electrolyte and even flames when subjected to extreme abuse. Manufacturers of these cells have gone to great lengths to incorporate multiple protection mechanisms to prevent such catastrophic failure. For example, advanced Li-ion cells incorporate both an internal circuit breaker and a separator material between the electrodes that blocks the transmission of electrons above a certain temperature to prevent thermal runaway (Cousseau et al 2005).

Another drawback that Li-ion cells share with all batteries is the loss of capacity over time. Capacity fade is dependent on the temperatures to which the cells are subjected and the depth-of-discharge of each cycle; higher temperatures and deeper cycles tend to reduce cell capacity over time (Bloom et al. 2001; Stamps et al. 2005; Liaw et al. 2005). However, at relatively shallow charge-discharge cycles, some Li-ion cells have exhibited no appreciable reduction in capacity over 80,000 cycles (Broussely 1999). Finally, Li-ion cells generally sell at a 60% premium over other secondary batteries due to the cost of materials. Because of their potential catastrophic failure mode, capacity fade, and initial expense, sophisticated battery management techniques are required to ensure the safety and efficacy of Li-ion cells over their useful life (Baker and Benstead 2005).

In spite of their shortfalls, Li-ion batteries have recently been employed in applications such as hybrid-electric vehicles, satellites, aircraft power systems, and stationary power storage (Gao, Liu, and Dougal 2002; Saft et al 1999). Further, recent reports from French battery maker Saft indicate that large packages of Li-ion cells, the “Dauphine” modules, are being evaluated for a notional AES energy storage application (Pelletier and Pommereau 2005). Recent publications support this assertion and indicate that the Navy is seeking to increase the durability and safety of Li-ion cells so that they may be incorporated into naval applications such as unmanned underwater vehicles in the near future (Govar and Banner 2003; Govar and Squires 2001).

A simple algebraic model was developed to determine the volume and mass of an ESM relying on Li-ion batteries. The model makes use of manufacturer data for the Saft high-power VL30P cell, including cell energy content, nominal power output, dimensions, and mass (Saft Batteries 2006). This particular cell was selected because it exhibits a balance between power output and energy content that makes it appropriate for the AES. This cell, or one that has very similar characteristics, is believed to be the constituent cell of the Dauphine modules (Pelletier and Pommereau 2005). A

commercially available cell was chosen in the spirit of the Navy’s focus on utilizing commercial-off-the-shelf (COTS) components whenever possible, especially for electrical components, to reduce the acquisition cost of the AES (Govar and Squires 2001; Thames 1998).

The Li-ion battery model calculates the number of cells needed to fulfill a specified peak-power and total energy demand. The battery system total volume and weight are then calculated based on the manufacturer’s data for a single cell, with correction factors accounting for cooling passages and packaging. The correction factors were quantified by comparing the model results to the known parameters of the Dauphine module (Saft Batteries 2005). For example, the Dauphine module is known to be composed of eighty cells. A module composed of eighty VL30P cells would have a total energy content of approximately 8.5 kW-hr, which compares favorably with the quoted value of 9 kW-hr. Incorporating a fifteen and thirty-five percent correction factor for volume and mass, respectively, results in the quoted Dauphine volume of sixty liters and mass of 120 kg.

Flywheels

Flywheels store energy in the rotation of a cylindrical rotor. A combined motor/generator acts as a motor to accelerate the rotor as energy is stored and a generator as energy is extracted. Input and output power electronics condition and control the signal as needed. Although the general concept of storing energy in a rotating mass has existed for over a century, several relatively recent technology innovations have led to the resurgence in interest in flywheel technology. The developments of low-loss magnetic bearings, the combined motor/generator, compact vacuum systems, and high-tensile strength composite fibers have created new opportunities and applications for flywheel energy storage (Bitterly 1998). In fact, flywheel designers can now optimize systems for high-power applications such as hybrid electric vehicles or high-energy applications such as utility energy storage and load leveling (Grudkowski et al 1996; Nourai 2002).

The major advantages that flywheels exhibit over electrochemical cells is high specific power, simple capacity monitoring, and a lifetime that is nearly independent of depth of discharge (Hebner, Beno, and Walls 2002). The power output of a flywheel is limited only by the capability of the power electronics. Capacity of a flywheel system is a simple function of rotational velocity, making knowledge of the state-of-charge significantly easier than for batteries. Finally, flywheels can have useful lifetimes of greater than twenty years, which helps to amortize their higher initial expense through reduced replacement costs.

The main drawback to flywheel energy storage has traditionally been low energy density, somewhat due to the required auxiliary equipment and power electronics. However, with the evolution of high-strength composite materials from which to form the rotating mass, flywheel systems with low inertia, high-velocity rotors have been built exhibiting significantly increased total stored energy (Bitterly 1998). However, these higher speeds are accompanied by increased safety issues associated with flywheels, with the worst being catastrophic disintegration of the rotor. Further, higher speeds create larger gyroscopic forces as energy is introduced and extracted from the flywheel. These complications can be dealt with, but the solutions inevitably increase the volume, mass, and complexity of a flywheel system.

For this analysis, a flywheel design was selected from the literature to represent the flywheel-based ESM (Hebner, Beno, and Walls 2002). This particular design was selected due to being optimized for a hybrid combat vehicle, which has requirements similar to the AES such as minimized mass and volume, high durability and robustness, and relatively high continuous power output. The flywheel is designed to store 25 MJ of energy, deliver 350 kW of continuous power, and has a rotor mass of 280 kg. A flywheel designed specifically for the AES from the literature was not selected due to a lack of sufficient data (McGroarty et al 2005).

Using methodology similar to the battery model, the flywheel ESM model calculates the number

of flywheels required to meet a given energy and peak-power demand. Through back calculations, the moment of inertia, diameter, height, and finally volume of the flywheel system were determined from the known parameters. The rotor material was assumed to be T-1000 graphite since the source only listed the material as composite/metallic. Mass and volume correction factors of sixty and 180 percent, respectively, were incorporated to account for the flywheel containment and auxiliary systems such as the power electronics package, health monitoring instrumentation, heat exchanger, and touchdown bearings (Bitterly 1998).

AES ENERGY, PEAK-POWER NEEDS AND LOAD PROFILES

Estimating Energy and Peak-Power Needs

Proper sizing of the ESM depends on accurately estimating total energy and peak-power requirements for the AES. Here, previous work from the literature provided significant insight into the loads the ESM would be expected to support, as well as the timeframe over which the ESM would need to function. The AES system demands during a dark-start emergency have historically been quantified through several discrete levels of power and operational time (Hudson and Ross 1998; Lipscombe, Davies, and Bolton 1998). These two specifications appear to have been chosen because they facilitate system-level calculations. Although other techniques exist in the literature, the conventional methodology has been to determine a minimum amount of time that stored energy might be required and multiply this by the nominal power that would be demanded over that timeframe (Amy 2002; van der Nat 1998).

At the critical power level, only ship systems that are absolutely critical to the safety of the ship and crew are provided power. At this level, it has been argued that the ESM must be able to supply uninterrupted power for a minimum of ten minutes to systems such as navigation and radar, ship steering (assuming it is electrically actuated), and emergency lighting (Hudson and Ross 1998; Lipscombe, Davies, and Bolton

1998). The ESM must also be able to provide enough power for several attempted startups of the GTGS, to mitigate the risk of a mechanical malfunction with any one particular unit. The GTGS startups represent a load on the ESM because, in the spirit of eliminating most hydraulic and pneumatic systems on board future ships, the gas turbines will probably be started electrically (McGroarty et al 2005; Newell, Mattick, and Hodge 1999). Adding an experimentally determined peak-power demand for a gas turbine electric start of 300 kW to a nominal power requirement of 350 kW creates a peak-power demand of 650 kW at the critical level (McGroarty et al 2005; Lipscombe, Davies, and Bolton 1998).

At the essential power level, all of the critical loads will be supplied along with other “services and equipments [that] preserve the normal functions and operations of the ship” (Hudson and Ross 1998). Despite a wider range of operation, this power level still excludes most domestic service, minor equipment, and propulsion. However, this level would undoubtedly provide for some minimal combat systems. The essential power level has been estimated to require a nominal power of about 1.1 MW (Hudson and Ross 1998). Adding the additional load of a gas turbine electric start results in a peak-power demand of 1.4 MW.

The propulsion power level allows for some limited maneuvering of the ship in addition to the essential load. References vary on reasonable speed and time requirements, but here it will be assumed that the ESM should be able to provide for a maximum ship speed of about 12 knots for a minimum of ten minutes (Lipscombe, Davies, and Bolton 1998; Hudson and Ross 1998; Hodge and Mattick 1995). Thus the propulsion power level has been estimated to be about 2.0 MW and model-based propulsion data for the DD(X) ship supports this estimate (Syntek Technologies 2003). The addition of a gas turbine start to this value results in a peak power demand of 2.3 MW.

AES Load Profiles

Uncertainty in the estimated energy and peak-power needs of the AES and the desire for a

robust ESM that can perform well across a variety of situations led to the creation of four different power-versus-time load profiles. The baseline profile, denoted “case-4,” was simply three gas turbine electric starts superimposed on the nominal power demand; the number of gas turbine starts was selected to simulate several failed startup attempts (Hudson and Ross 1998). The shape of the gas turbine startup power demand was designed to approximate experimental results from the literature (McGroarty et al 2005). A MATLAB script was written to calculate the total energy consumed by the AES during the ten-minute timeframe. For example, the critical power level of 350 kW and three gas turbine startups results in a peak-power demand of 650 kW and a total energy demand of approximately 65 kW-hr, as shown in Figure 2.

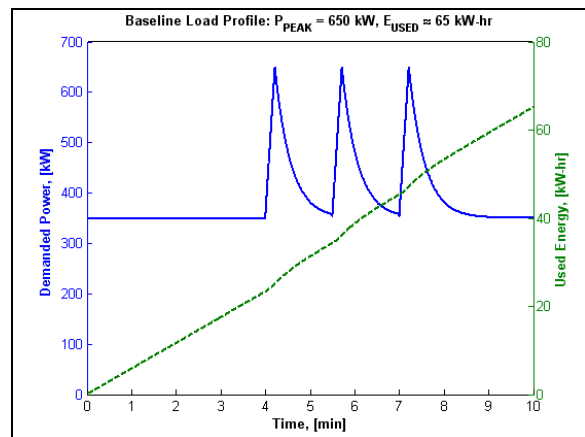


FIGURE 2. Case-4, Baseline Load Profile at Critical Power Level.

The other load profiles were created to simulate uncertain load situations that might be faced during a real dark-start emergency. Case-1 simulated a relatively stable, or flat-topped, load profile with large power ramp-ups and ramp-downs at the beginning and end of the timeframe, as shown in Figure 3. Case-2 represented a simple sinusoidal load profile, as shown in Figure 4. Finally, Figure 5 shows the case-3 load profile that simulated a nominal power demand oscillating about a mean. The nominal power of each of the three additional load profiles was modulated to ensure that the total energy consumed during the timeframe would equal that of the baseline case.

Consequently, each load profile had a different peak power.

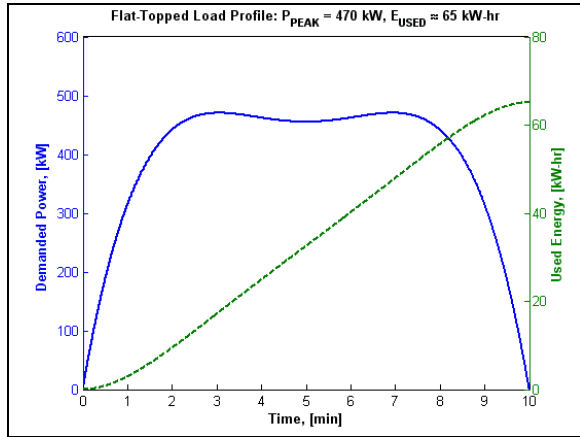


FIGURE 3. Case-1, Flat-Topped Load Profile at Critical Power Level.

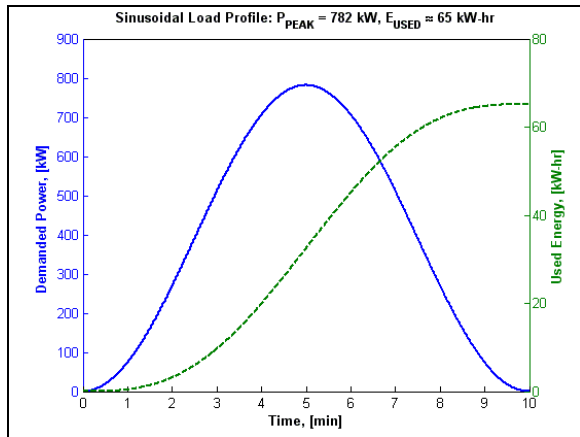


FIGURE 4. Case-2, Sinusoidal Load Profile at Critical Power Level.

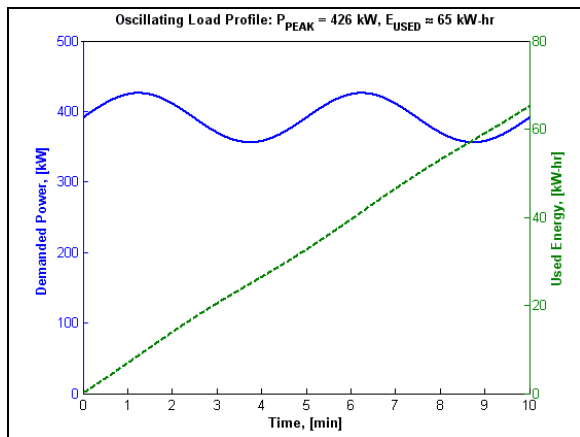


FIGURE 5. Case-3, Oscillating Load Profile at Critical Power Level.

PRELIMINARY RESULTS AND OPTIMIZATION FORMULATION

Calculations of the mass and volume of an ESM composed solely of flywheels or Li-ion batteries are presented in Tables 1 and 2, respectively. These preliminary results show that an ESM supplying the demanded total energy and peak-power for each load profile, power level combination while having a minimum system mass and volume would be composed solely of Li-ion batteries. Further, a robust design that could meet the requirements of any case at a particular power level would be designed to meet the needs of case-2, due to that case having the highest peak-power. Finally, the overall robust solution that could supply energy and peak-power for any load profile at any power level would be the ESM design for case-2 at the propulsion power level. This system would be composed of nearly 6,400 Li-ion cells, have a mass of 10.5 U.S. tons, and a volume of nearly five cubic meters.

TABLE 1 Flywheel ESM Characteristics

Load Profile #	Peak Power [kW]	Flywheels		
		Number Flywheels	Weight [ton]	Volume [m ³]
Critical Power Level (65 kW-hr)				
1	470	10	3.1	9.1
2	782	10	3.1	9.1
3	426	10	3.1	9.1
4	650	10	3.1	9.1
Essential Power Level (190 kW-hr)				
1	1,373	28	13.8	25.4
2	2,282	28	13.8	25.4
3	1,243	28	13.8	25.4
4	1,400	28	13.8	25.4
Propulsion Power Level (340 kW-hr)				
1	2,456	49	24.2	44.4
2	4,082	49	24.2	44.4
3	2,223	49	24.2	44.4
4	2,300	49	24.2	44.4

TABLE 2 Battery ESM Characteristics

Load Profile #	Peak Power [kW]	Batteries		
		Number Cells	Weight [ton]	Volume [m ³]
Critical Power Level (65 kW-hr)				
1	470	736	1.2	0.6
2	782	1,224	2.0	0.9
3	426	667	1.1	0.5
4	650	1,017	1.7	0.8
Essential Power Level (190 kW-hr)				
1	1,373	2,149	3.5	1.6
2	2,282	3,572	5.9	2.7
3	1,243	1,946	3.2	1.5
4	1,400	2,191	3.6	1.6
Propulsion Power Level (340 kW-hr)				
1	2,456	3,844	6.3	2.9
2	4,082	6,389	10.5	4.8
3	2,223	3,479	5.7	2.6
4	2,300	3,600	5.9	2.7

The results indicate that, with the selected flywheel design, the number of flywheels in the ESM is dictated solely by the energy demand, independent of the peak-power requirement. Conversely, the peak-power determined the number of battery cells that would compose the ESM. These results fit with the general view that flywheels are power dense while batteries are energy dense.

The results may be skewed away from flywheels due to the rather large correction factors for mass and volume of the flywheel that were used. However, without improved flywheel data to refute the assumed values, these factors were not altered. Despite that complication, the results indicate that the Li-ion cells are nearly optimal for the operational needs set out in this study. Although not shown in Table 2, the number of cells required to meet the energy or peak-power requirements of the ship were very nearly equal for all but the highest peak-power cases at each power level

Optimization Formulation

Several previous assessments of the energy storage options for the AES speculated that a hybridized battery-flywheel ESM might be the optimal solution (Lipscombe, Davies, and

Bolton 1998; Donaldson 2002). In this vein, the Ministry of Defense in the United Kingdom utilized a battery-flywheel hybridized ESM in their Electric Ship Technology Demonstrator (Little and Norton 2003; Longepe and Smith 2002; Young, Newell, and Little 2001). To test the hypothesis that a hybrid system might be able to meet the energy and peak-power needs of the AES and result in an ESM with a minimum mass and volume, an objective function that represents the mass, volume, and peak-power capability of each hybrid design was created.

The optimization seeks to minimize the metrics of system mass, volume, and power deficiency (PD) across all four cases at each power level. PD is defined here as the sum across the four cases of the difference between peak power demanded, as indicated on load profile plots such as Figures 2 through 5, and peak-power supplied by the tested ESM. PD was created to help quantify how robust an ESM design would be across all of the load profile cases. PD was only calculated if the power supplied by the ESM was less than the demanded power; otherwise, it was zero. Therefore, designs were not punished for providing a peak-power higher than that demanded by a particular load profile. The objective function was formed using the Weighted Least Squares Method, as shown in Equation 1:

$$Z = \left\{ \sum_{i=1}^m [w_i \cdot (f_i(n_{FW}, n_B) - f_i^*)]^2 \right\}^{\frac{1}{2}} \quad (1)$$

where:

- n_{FW}, n_B are the number of flywheels and batteries, respectively,
- $f_i(n_{FW}, n_B)$ is the normalized system mass, volume, or PD for each design,
- f_i^* is the normalized target value for each metric, and
- w_i is the assigned weight of importance for each metric.

The target values are the minimum possible values of mass, volume, and PD of designs that meet the system energy and power needs. The target value for metric i was determined by

optimizing the ESM with w_i equal to unity. Note that, like all weighted methods, the sum over i of w_i was always equal to unity.

The multiobjective optimization problem is formulated as shown in Figure 6. The constraints force each ESM design to meet, at a minimum, the energy and peak-power needs of the case-4 load profile. Preference was shown to case-4 because it is supported by the literature. For the load profile in Figure 2, for example, E_{stored} and $P_{delivered}$ are required to meet or exceed 65 kW-hr and 650 kW, respectively.

$$\begin{aligned} & \text{Minimize } Z = \left\{ \sum_{i=1}^m [w_i \cdot (f_i(n_{FW}, n_B) - f_i^*)]^2 \right\}^{\frac{1}{2}} \\ & \text{Subject to} \\ & \quad E_{stored} \geq \bar{E}_{stored, case-4} \\ & \quad P_{delivered} \geq \bar{P}_{peak, case-4} \\ & \quad n_B^L \leq n_B \leq n_B^U \\ & \quad n_{FW}^L \leq n_{FW} \leq n_{FW}^U \end{aligned}$$

FIGURE 6. Optimization Problem Formulation

The design variables are assigned upper bounds, n_B^U and n_{FW}^U , and lower bounds, n_B^L and n_{FW}^L .

These ranges reduce the design space over which the optimization algorithm searches, decreasing computation time. The number of batteries is normalized in practice to reduce its magnitude to a range similar to that of n_{FW} and thereby facilitate the optimization search process. For example, at the critical power level the number of flywheels, n_{FW} , is permitted to vary from zero to two, and the normalized number of batteries, n_B , between two and ten. These bounds were created after preliminary calculations showed no optimal solutions existed outside of these ranges.

Since the contribution of a single flywheel to the objective function is large relative to that of a single battery, n_{FW} is treated as an integer while n_B is treated as a continuous variable. This results in a mixed-integer programming problem. Consequently, the Branch and Bound

Method is used to optimize the system configuration (Belegundu and Chandrupatla 1999).

HYBRID ESM RESULTS

The Branch and Bound algorithm optimized the objective function by varying n_{FW} and n_B for specific, user-defined combinations of weights, (w_M, w_V, w_{PD}) . Plots of results for the critical and essential power levels are shown in Figures 7 and 8, respectively.

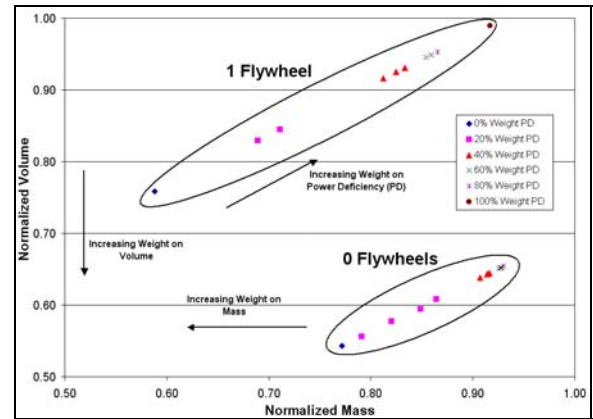


FIGURE 7. Optimal Hybrid ESM Characteristics at Critical Power Level.

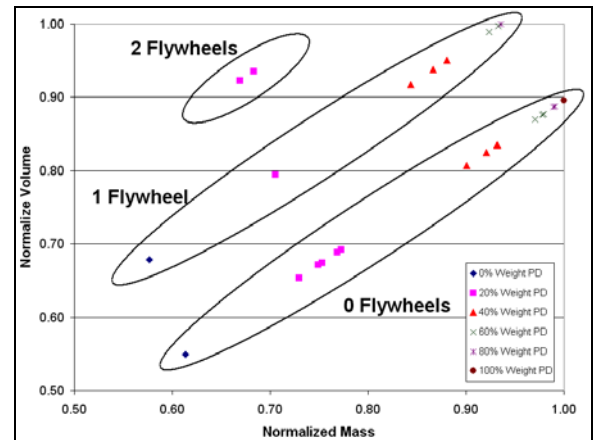


FIGURE 8. Optimal Hybrid ESM Characteristics at Essential Power Level.

Weights were varied to produce a range of potential ESM hybrid systems that met all of the constraints, but represented a range of tradeoffs between the objectives of mass, volume, and robustness. As depicted in the figures, the weight on PD was varied from 0 to 100%. Solutions for each weighting of PD are indicated

by distinct symbols. More than one solution is reported for each weighting of PD because the remaining weight is distributed between mass and volume in several different allocations (e.g., 20% PD, 0% mass, 80% volume; 20% PD, 40% mass, 40% volume).

The results in the upper region of Figure 7 represent optimized ESM designs consisting of one flywheel and various numbers of Li-ion batteries. The lower region represents designs consisting of only Li-ion batteries. Figures 7 and 8 together illustrate that even high-power situations require the use of, at most, two flywheels. The results for the propulsion power level are not presented because they are very similar to the results for the essential level. Note that the results shown in Figures 7 and 8 are normalized by different factors, due to each power level having different total energy and peak-power requirements.

As shown in Figure 7, higher weights on PD lead to bulkier, heavier ESM designs as additional batteries are added to prevent power deficiencies at the highest peak power levels. As the weight on mass is increased for constant weight on PD, the ESM designs become lighter and more compact until the relative weight on volume becomes so small that a flywheel is inserted. The insertion of a flywheel—as depicted by a jump from the lower to the upper region of the plot—reduces mass but increases volume relative to the batteries it replaces. In general, the hybridized ESM designs tend to have smaller system mass but larger system volume than corresponding battery-only designs.

Figures 9 and 10 show plots of ranges of system mass and volume, respectively, for different values of w_{PD} at the critical power level. As expected, the mass and volume of the ESM increase with w_{PD} , because the system supplies more peak-power. The range of potential system masses decreases while the magnitudes increase with increasing w_{PD} . Additionally, the range of potential system volumes remains relatively constant while the magnitudes increase with increasing w_{PD} .

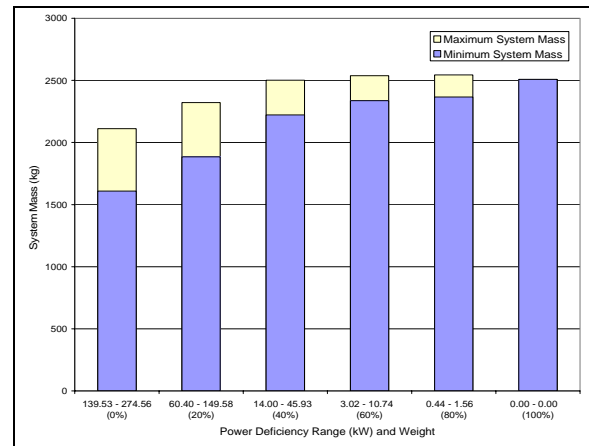


FIGURE 9. Range of ESM Mass as a Function of w_{PD} .

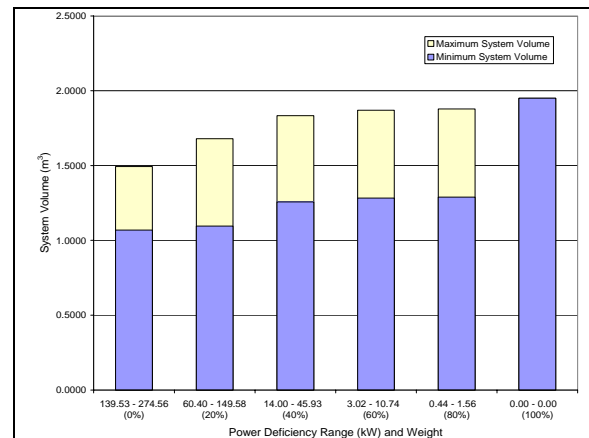


FIGURE 10. Range of ESM Volume as a Function of w_{PD} .

An engineer charged with designing the AES ESM would most likely be provided with limits of maximum allowable system mass and volume, expected nominal and peak-power, and maximum system cost. Knowledge of these would help the designer interpret a plot such as Figure 7. Maximum allowable system mass and volume would section the plot, allowing the designer to immediately identify several feasible solutions. The most robust design could then be found by identifying the design with the highest value of w_{PD} .

CONCLUSIONS

Based on an assessment of energy storage options for a future AES, Li-ion batteries and flywheels were identified as the most promising technologies for an AES ESM. If a single energy storage technology were chosen for the power levels and load distributions presented in this study, the ESM would be composed solely of Li-ion batteries, as seen by comparing the system characteristics in Tables 1 and 2. For such an ESM, the expected total energy and peak-power requirements govern the number of cells and the corresponding system weight and volume. The flywheel-only designs suffered from comparatively higher system mass and volume, possibly due to the conservative correction factors incorporated into the calculation.

As proposed in the literature, under some conditions a lower ESM mass can be achieved by incorporating flywheels. When identifying appropriate numbers of batteries and flywheels, the designer must negotiate tradeoffs between system mass, volume, and robustness, as quantified in PD. For a given total energy, peak-power, and maximum system mass and volume, sets of feasible designs can be generated using multiobjective optimization techniques. From plots of the designs, as shown in Figures 7 and 8, a designer can visualize the range of feasible tradeoffs and select an appropriate design based on relevant criteria, such as the most robust design with the highest value of w_{PD} that satisfies maximum mass and volume limits.

A major weakness in this study is the inherent subjectivity of the assessment of energy storage options of the AES, which may have resulted in the selection of technologies that were not truly feasible or the elimination of some technologies that were. Additionally, a lack of detailed data for the modeled Li-ion cell and flywheel forced the adoption of assumed mass and volume correction factors, which may have unfairly skewed the results toward Li-ion cells. Finally, the lack of realistic load profiles combined with the desire to create robust solutions led to the creation of three arbitrary load profiles. Optimizing the ESM to meet the needs of these

load profiles may have significantly affected the results. In spite of these weaknesses, the authors remain confident in the methodology used throughout this study, and hope the AES community finds the results relevant and useful.

REFERENCES

- Amatucci, G.G. and F. Badway, "Nanotechnology—Enabler of Next Generation Energy Storage?," *International Energy Conversion Engineering Conference (IECEC)*, Paper No. 20184, 2002.
- Amy, J.V., "Considerations in the Design of Naval Electric Power Systems," *Proceedings of the 2002 IEEE Power Engineering Society Summer Meeting*, pp. 331-335, 2002.
- Baker, J.N. and N. Benstead, "Bulk Energy Storage Systems for the Royal Navy," *All Electric Ship: Developing Benefits for Maritime Applications*, 2005.
- Barker, P.P., "Ultracapacitors for Use in Power Quality and Distributed Resource Applications," *2002 IEEE Power Engineering Society Summer Meeting*, pp. 316-320, 2002.
- Belegundu, A.D. and T.R. Chandrupatla, *Optimization Concepts and Applications in Engineering*, Prentice Hall, Upper Saddle River, NJ, 1999.
- Bitterly, J.G., "Flywheel Technology: Past, Present, and 21st Century Projections," *IEEE Aerospace and Electronic Systems Magazine*, v. 13, n. 8, pp. 13-16, August 1998.
- Bloom, I., B.W. Cole, J.J. Sohn, S.A. Jones, E.G. Polzin, V.S. Battaglia, G.L. Henriksen, C. Motloch, R. Richardson, T. Unkelhaeuser, D. Ingersoll, and H.L. Case, "An accelerated calendar and cycle life study of Li-ion cells," *Journal of Power Sources*, Vol. 101, pp. 238-247, 2001.
- Broussely, M., "Recent development on lithium ion batteries at SAFT," *Journal of Power Sources*, vol. 81-82, pp. 140-143, 1999.

- Cousseau, J.F., C. Siret, P. Biensan, and M. Broussely, "Recent developments in Li-ion prismatic cells," *Journal of Power Sources*, article in press at the time of this writing, 2005.
- Doerry, N.H. and J.C. Davis, "Integrated Power System for Marine Applications," *Naval Engineers Journal*, Vol. 106, Issue 3, pp. 77-90, May 1994.
- Doerry, N.H., H. Robey, J. Amy, and C. Petry, "Powering the Future with the Integrated Power System," *Naval Engineers Journal*, Vol. 108, Issue 3, pp.267-282, May 1996.
- Donaldson, A.J., "Energy Storage – new technologies and new roles," *in ec 2002: The Marine Engineer in the Electronic Age - Conference Proceedings*, pp. 237-245, April 23-25, 2002.
- Donaldson, A.J. and D. Williamson, "Advanced Batteries: New Capability for an Electric Ship," *All Electric Ship: Developing Benefits for Maritime Applications*, 2005.
- Dustmann, C.H., "Advances in ZEBRA batteries," *Journal of Power Sources*, vol. 127, pp. 85-92, 2004.
- Ewing, D.L., R.W. Holmes, B.G. Rochon, J.B. Daley, and T.T. Hellman, "A Surface Combatant for the 21st Century: DDG 51 Flight IIA," *Naval Engineers Journal*, pp. 217-232, May 2005.
- Gao, L., S. Liu, and R.A. Dougal, "Dynamic Lithium-ion Battery Model for System Simulation," *IEEE Transactions on Components and Packaging Technologies*, Vol. 25, No. 3, September 2002.
- Govar, C.J. and J.A. Banner, "Safety Testing of Lithium Ion Batteries for Navy Devices," *IEEE Aerospace and Electronics Systems Magazine*, Vol. 18, no. 1, pp. 17-20, January 2003.
- Govar, C.J. and T.L. Squires, "Safety Tests of Lithium 9-Volt Batteries for Navy Applications," *Proceedings of the 16th Annual Battery Conference on Applications and Advances*, pp. 337-341, January 2001.
- Grudkowski, T.W., A.J. Dennis, T.G. Meyer, P.H. Wawrzonek, "Flywheels for Energy Storage," *SAMPE Journal*, v. 32, n. 1, pp. 65-69, January-February, 1996.
- Hebner, R., J. Beno, and A. Walls, "Flywheel Batteries Come Around Again," *IEEE Spectrum*, pp. 46-51, April 2002.
- Hodge, C.G. and D.J. Mattick, "The electric warship," *Transactions of the Institute of Marine Engineering (IMarE)*, Vol. 108, Part 2, pp. 109-125, 1995.
- Hudson, R.P.M. and C.M. Ross, "The cost benefits of single generator operation through the use of energy storage devices on warships," *All Electric Ship: Developing Benefits for Maritime Applications, AES1998*, Session 12, Paper I, pp. 191-200, 29-30 September 1998.
- Liaw, B.Y., R.G. Jungst, G. Nagasubramanian, H.L. Case, and D.H. Doughty, "Modeling capacity fade in lithium-ion cells," *Journal of Power Sources*, Vol. 140, pp. 157-161, 2005.
- Lipscombe, R.S., C.P. Davies, and M.T. Bolton, "Energy Storage in the all electric ship," *All Electric Ship: Developing Benefits for Maritime Applications, AES1998*, Session 12, Paper II, pp. 201-206, 29-30 September 1998.
- Little, G.T., S.S. Young, and J.M. Newell, "The electric warship VII – the reality," *Journal of Marine Design and Operations*, 2001.
- Little, G.T. and P. Norton, "Demonstrating the Electric Ship," *Naval Engineers Journal*, v. 115, n. 4, pp. 91-105, Fall 2003.
- Longepe, B. and N. Smith, "De-risking the electric ship: from theory to reality," *INEC 2002*, Glasgow, UK, 23-25 April 2002.
- McCoy, T.J., "Trends in Ship Electric Propulsion," *2002 IEEE Power Engineering Society Summer Meeting*, pp. 343-346, 2002.
- McGroarty, J., J. Schmeller, R. Hockney, and M. Polimeno, "Flywheel Energy Storage System for

Electric Start and an All-Electric Ship,” *Proceedings of the 2005 IEEE Electric Ship Technologies Symposium*, pp. 400-406, 25-27 July 2005.

Newell, J.M., D.J. Mattick, and C.G. Hodge, “The Electric Warship IV,” *Transactions of the IMarE*, Vol. 111, Part 1, pp. 25-30, 1999.

Newell, J.M. and S.S. Young, “Beyond Electric Ship,” *International Maritime Technology*, Vol. 113, n 1, pp. 13-23, 2001.

Nourai, A., “Large-Scale Electricity Storage Technologies for Energy Management,” *2002 IEEE Power Engineering Society Summer Meeting*, pp. 310-315, 2002.

Pelletier, J. and Y. Pommereau, “Lithium Ion Naval Energy Storage Systems (NESS),” *All Electric Ship: Developing Benefits for Maritime Applications*, 2005.

Price, A., “Energy Storage, an unconventional renewable?,” *IEE Colloquium (Digest)*, n. 205, pp. 33-36, Nov. 1999.

Saft Batteries, “All Electric Ships,” website at http://www.saftbatteries.com/060-MS_Military/50-20-30_All_electric_ship.asp, accessed 15 November 2005.

Saft Batteries, “Lithium systems, VLP cells, More Information,” online product documentation available at http://www.saftbatteries.com/120-Techno/20-10_produit.asp?sSegment=&sSegmentLien=&sSecteurLien=&ssecteur=&Intitule_Produit=VLPcells&page=2, accessed 07 February 2006.

Saft, M., G. Chagnon, T. Faugeras, G. Sarre, and P. Morhet, “Saft lithium-ion energy and power storage technology,” *Journal of Power Sources*, vol. 80, pp.180-189, 1999.

Schinker, R.B., “Executive Overview: Energy Storage Options for a Sustainable Energy Future”, *2004 IEEE Power Engineering Society*

General Meeting, v.2, pp. 2309-2314, June 2004.

Sette, K. and J. Spina, “Energy Storage for Large Scale Vehicles,” *Proceedings of the IEEE Symposium on Autonomous Underwater Vehicle Technology*, pp. 19-25, 2002.

Stamps, A.T., C.E. Holland, R.E. White and E.P. Gatzke, “Analysis of capacity fade in a lithium ion battery,” *Journal of Power Sources*, Vol. 150, pp. 229-239, 2005.

Surko, S. and M. Osbourne, “Operating Speed Profiles and the Ship Design Cycle,” *Naval Engineers Journal*, Vol. 117, Issue 3, pp. 79-85, Summer 2005.

Syntek Technologies, “DD(X) Notional Baseline Modeling and Simulation Development Report in Support of the Electric Ship Research and Development Consortium,” intra-Consortium document, 1 August 2003.

Szymborski, J., “Lead-acid batteries for use in submarine applications,” *Proceedings of the IEEE Symposium on Autonomous Underwater Vehicle Technology*, pp. 11-17, 2002.

Thames, T., “Using Commercial Off-The-Shelf (COTS) Equipment to Meet Joint Service Requirements,” *1998 IEEE AUTOTESTCON Proceedings*, pp. 204-209, 1998.

van der Nat, J.M. and D. Stapersma, “Application of battery cells onboard merchant ships,” *All Electric Ship: Developing Benefits for Maritime Applications, AES1998*, Session 12, Paper III, pp. 207-215, 29-30 September 1998.

Young, S., J. Newell, and G. Little, “Beyond Electric Ship,” *Naval Engineers Journal*, vol. 113, n. 4, pp. 79-92, Fall 2001.

ACKNOWLEDGEMENTS

This work was sponsored by the Office of Naval Research under the auspices of the Electric Ship Research and Development Consortium.